A method for splitting digital value in radiological image compression

Shih-Chung B. Lo
Radiology Department, Georgetown University, Washington, DC 20057

Ellen L. Shen
Mathematics Department, Massachusetts Institute of Technology, Cambridge, Massachusetts 02139

Seong K. Mun
Radiology Department, Georgetown University, Washington, DC 20057

Ji Chen
Department of Electrical Engineering, University of Michigan, Ann Arbor, Michigan 48109

(Received 20 July 1990; accepted for publication 2 January 1991)

A new decomposition method using image splitting and gray-level remapping has been proposed for image compression, particularly for images with high contrast resolution. The effects of this method are especially evident in this radiological image compression study. In these experiments, the impact of this decomposition method was tested on image compression by employing it with two coding techniques on a set of clinically used CT images and several laser film digitized chest radiographs. One of the compression techniques used as zonal full-frame bit-allocation in the discrete cosine transform (DCT) domain, which is an enhanced full-frame DCT technique that has been proven to be an effective technique for radiological image compression. The other compression technique used was vector quantization with pruned tree-structured encoding, which through recent research has also been found to produce a low mean-square error and a high compression ratio. The parameters used in this study were mean-square error and the bit rate required for the compressed file. In addition to these parameters, the differences between the original and reconstructed images were presented so that the specific artifacts generated by both techniques could be discerned through visual perception.

Key words: image compression, image decomposition, and digital imaging

I. INTRODUCTION

Because it is apparent that more and more digital medical modalities will be used in the future, it is expected that a great deal of digital information will need to be stored and transmitted in a clinical environment.[1] In dealing with this, the issues of data storage and transmission speed must be addressed. It has been found that image data compression can be of great benefit in both of these areas. Among the many existing compression techniques, the techniques involving encoding in the discrete cosine transform (DCT) and vector quantization have been shown to be the most efficient in terms of compression ratio and reconstructed image quality. In this study, we applied the full-frame bit-allocation technique[2–4] (FFBA) in the DCT domain and the vector quantization with pruned tree-structured encoding (VQTSE) technique[5,6] to a number of medical images. The original images were preprocessed in such a way that the most significant three bits were retained using Lempel–Ziv[7] (LZ) coding (N.B. sole application of Huffman coding[8] is not suitable for this type of image), and the least significant nine bits were remapped to a new gray-level scale and then encoded by FFBA and VQTSE. The remapping method will be discussed in further detail in Sec. II. The results of the compression studies will be revealed in later sections.

II. MATERIALS AND METHODS

We acquired 22 clinical CT abdominal images, 1 CT head image, and 8 chest radiographs digitized by a laser film scanner. The CT images consisted of $512\times512\times12$ bits, and the chest images were digitized at $2048\times2300\times12$ bits and miniaturized to $1024\times1024\times12$ bits (chest 1–7). One chest image was shrunk to $512\times512\times12$ bits (chest 1). All images were randomly selected from our clinical patient database.

A. Image splitting and remapping

In medical imaging, a high correlation in the top two to three most significant bits (MSB) has been found.[9] This characteristic is favorable to correlation encoding (e.g., LZ coding and run-length/Huffman coding); a high-compression ratio can be expected. The application of a transform coding to the MSB image, on the other hand, will not produce good results, since the sharp-edge information is difficult to encode with wave-based coding. Because of the different applications of the encoding techniques, we proposed splitting the image into two parts and subsequently encoding each part using a different coding process. For example, one could encode the MSB image with LZ coding and the least

 0094-2405/91/050939-08$01.20

TABLE I. Remapped values from the splitting and remapping method.

Original value	3MSB	9LSB	R9LSB
0–511	0	0–511	0–511
512–1023	1	0–511	511–0
1024–1535	2	0–511	0–511
1536–2047	3	0–511	511–0
2048–2559	4	0–511	0–511
2560–3071	5	0–511	511–0
3072–3583	6	0–511	0–511
3584–4095	7	0–511	511–0

significant bit (LSB) image with FFBA. We believed that this splitting method would also be suitable for LZ coding and VQ. The reason for this is that the splitting method produces less variation in the image and thus less variety in the codebook of the VQ library, making encoding more accurate. The method of splitting the image into two parts is trivial. The operation that remaps the J least significant bits (LSB) for image $f(x,y)$ can generally be expressed by

$$\begin{aligned} &\mathrm{LSB}_J(f(x,y)), \quad \text{for } (f(x,y)\&2^J)=0, \\ &\mathrm{RLSB}_J(f(x,y)) \\ &\quad = 2^J-1-\mathrm{LSB}_J(f(x,y)), \quad \text{for } (f(x,y)\&2^J)\neq 0, \end{aligned} \tag{1}$$

where J represents the number of LSB and "&" is the "AND" operation for bit map.

In our experiments, the procedure consisted of first separating the top three MSB of the image from the original image. Based on (1), the residual image containing the nine LSB was then remapped according to the values shown on Table I, where 3MSB are the 3 most significant bits, 9LSB are the 9 least significant bits, and R9LSB denotes the remapped 9 least significant bits. The purpose of remapping was to try to convert the residual data into an image with a more continuous tone, which would in turn lead to greater compression.

The 3MSB image was decomposed with the differential pulse code modulation method (DPCM), then encoded by LZ coding. The LZ encoder uses a data dictionary of strings and string codes to parse image data values into strings of pixel values. The data dictionary is derived as the data encoding is running, which makes an external codebook unnecessary. Output codes are produced from the parsed strings. Decompression then consists of using a lookup table to generate strings represented by code words. With highly correlated data, the LZ algorithm achieves a high compression that is sometimes superior to the simple entropy encoding. In fact, in our initial experiments, we found that high compression (7:1 to 15:1) can be obtained in the top two to four MSB images without distortion. The initial experiments covered 200 CT, 200 MR, and 50 digital radiographs from a laser digitizer in our Picture Archiving and Communication System (PACS) database. The 15:1 compression ratio was found in the group of lateral view chest radiographs with 2MSB. The 7:1 compression ratio was found in some of the CT head images (between eye and mouth levels) with 4MSB. The residual remapped LSB image contains detailed structure,[10] with less sharp-edge quality and lower bit values, which we expected would be more compressible with FFBA or VQTSE techniques.

In summary, the reason for using the splitting technique is twofold: (a) the extremely high correlation of a MSB image provides for a high compression ratio with error-free compression, and (b) the correlation near the edges of the RLSB image is improved.

B. A practical FFBA algorithm—zonal FFBA

The decomposition of FFBA is obtained by a two-dimensional discrete cosine transform (2-D–DCT), and the encoding is done by quantization and bit-allocation techniques.[2,4] Each value in the bit allocation table (BAT) points to an area of the 2-D–DCT region (e.g., 2×2 pixels). The BAT can later be compressed by error-free coding (e.g., Huffman coding). Each frequency amplitude value in the 2-

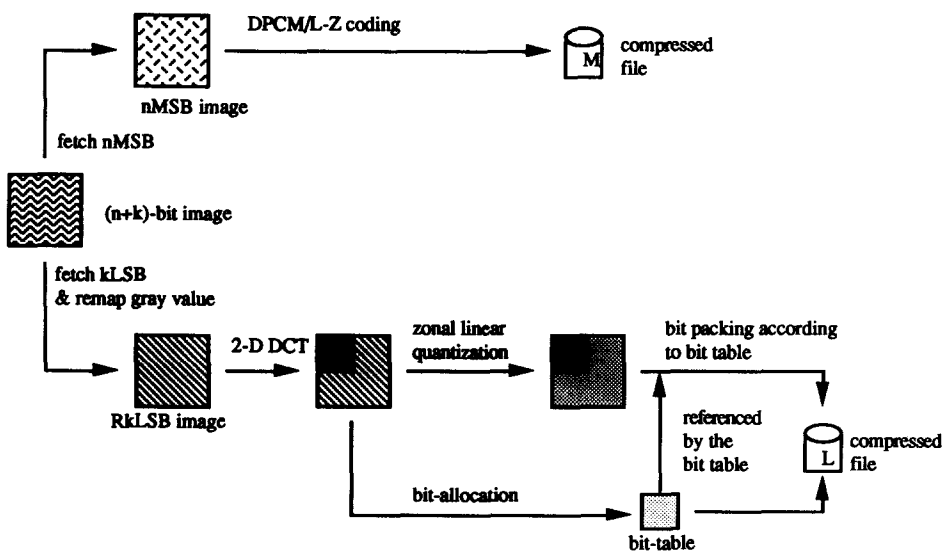

FIG. 1. Zonal full-frame bit-allocation compression technique with splitting method.

D–DCT matrix is quantized. An example of such a quantization is given below:

$$F_q(u,v) = \mathrm{NINT}(2^{[B(m,n)-1]} - 1)\, F(u,v)/|F(m,n)|, \quad (2)$$

where $F(u,v)$ is the frequency amplitude value of the 2-D–DCT; $Fq(u,v)$ is the corresponding quantized value; (m,n) is the location of the maximum value of $|F(u,v)|$ for $u,v = 0,...,N-1$; $B(m,n)$ is the corresponding number of bits in the BAT designated to save $|F(m,n)|$; and NINT is the nearest integer operator. In this formula, $F(u,v)$ has been normalized with respect to $(2^{[B(m,n)-1]} - 1)/|F(m,n)|$. In fact, F_q can be further compressed by Huffmann coding, which can improve the compression ratio by a factor of 1.5. This is discussed extensively in Ref. 4. However, the extra Huffman coding is not used in this paper.

The reverse quantization of (2) is shown below:

$$F_r(u,v) = |F(m,n)|\, F_q(u,v)/(2^{[B(m,n)-1]} - 1), \quad (3)$$

where $F_r(u,v)$ is the approximation of $F(u,v)$. The reconstructed image is obtained by applying an inverse 2-D–DCT to $F_r(u,v)$. The difference between $F(u,v)$ and $F_r(u,v)$ results from the inherent inaccuracy of quantization procedures (2) and (3). This also accounts for the differences between the original image $f(x,y)$ and the reconstructed image $f_r(x,y)$, since the energy is conserved in both the spatial and frequency domains, regardless of a unitary transform. This is described by Parseval's theorem:

$$\int\int f^2(x,y)dx\,dy = \int\int F^2(u,v)du\,dv. \quad (4)$$

From (2) and (3), it can be seen that the error is highly related to the value of $|F(m,n)|$. The smaller the value of $|F(m,n)|$, the smaller the resulting difference between $F(u,v)$ and $F_r(u,v)$. For continuous tone images, the largest value often occurs at $F(0,0)$ (i.e., the DC coefficient). Typically, the coefficients decrease rapidly by a two-dimensional exponential fall-off as the frequency is increased. A practical way of error justification is using the zone treatment. This method isolates the low, medium, and high frequency zones and linearly quantizes the respective coefficients in each zone. Theoretically, there can be as many zones as needed. In this study, three zones were used and separated at pixels 64 and 128 for a 1024×1024 square image to justify the overhead required in each zone and the quantization error. The maximum value of $|F(u,v,z)|$ for each zone $z = 1,2,3...$was then obtained for the quantization indicated in (2). In each zone, this value, $F(m,n,z)$, was saved in the compressed file for the reverse quantization given by (3). The proposed zonal FFBA algorithm is shown in Fig. 1.

C. Review of VQTSE[5,6]

The tree-structured VQ library is based on a "training sequence" of several images, and consists of a number of nodes branching off into left and right children nodes, starting with one root node at the top. Each node contains a library code word, which bears some similarity to a high percentage of vectors in the training sequence. Once the tree-structured library has been made, the pruning technique can be applied. This will create trees of varying height, resulting in a natural variable rate code. The advantage of this is that the encoder is then able to use more bits to code the high activity and high distortion regions, while using fewer bits for the low intensity or unimportant areas of the image, such as background. Pruned VQ has been proven to perform significantly better than the fixed-rate code of tree-structured VQ.[5,6]

The pruning algorithm finds subtrees (we shall denote one such subtree by S) of the total tree T. It does this by minimizing the function

$$F(S) = D(S) + \lambda L(S) \quad (5)$$

for all $S \leqslant T$. Here $D(S)$ denotes the average distortion obtained from using S as an encoder, and $L(S)$ represents the code word length. The parameter λ can be viewed as a Lagrange multiplier that trades off distortion for rate. We can represent λ by

$$\lambda = -|\Delta D(S)/\Delta L(S)|, \quad (6)$$

where $\Delta D(S)$ is the change in distortion, and $\Delta L(S)$ is the decrease in code word length resulting from pruning off a branch of T. Since λ thus measures the ratio of increase in distortion to decrease in rate brought about by pruning, higher values of λ (or equivalently, lower absolute values of λ, since λ is negative) are desired. Thus pruning consists of removing the nodes with the lowest values of λ from the tree to find the lower convex hull of the function

$$G(R) = \min_{S \leqslant T} [\, D(S) | L(S) \leqslant R \,], \quad (7)$$

where R represents the desired rate. The removal of each node results in a new pruned tree, optimal in that it gives the lowest average distortion of all subtrees with the same or a lesser average rate. The measure of distortion is determined by mean-square error (MSE/VQ) or by other modified distortion algorithms. In this study, the MSE/VQ algorithm was used.

D. Reconstruction image quality measurements

Mean-square error (MSE/Image or MSE), the parameter used to evaluate the quality of the reconstructed images, is a global measurement of distortion between original and reconstructed images. It is given by the following formula:

$$\mathrm{MSE} = \sum_x \sum_y [f(x,y) - fr(x,y)]^2/N, \quad (8)$$

where N = total number of pixels in the image. Since original CT images are formatted with 12 bits/pixel and within the central circular area, the MSE calculations of the CT images were confined to the interior of a circle 512 pixels in diameter. In this case N is 205 888 ($\approx 256\times256\times\pi$); this value was also used in the computation of the compression efficiency for the CT images in our study. The compression efficiency can be expressed as the average number of bits per pixel (or bit rate per pixel). This can be calculated by dividing the total number of bits required to store the compressed file by the number of pixels in the original file (N). The compression ratio, which is the ratio between the bit rate

required for the original file and the bit rate required for the compressed file, is another way of expressing the compression efficiency of a method.

Visual observations of both the reconstructed image and the image resulting from the subtraction of the reconstructed image from the original image were taken as well to ascertain the specific artifacts created in the reconstructed image. Each pixel in the difference image was enhanced by a factor of 50 in this paper. This difference image was calculated by

$$f_d(x,y) = (f(x,y) - f_r(x,y)) \cdot 50 + 2048. \quad (9)$$

A gray value of 2048 was added to the difference values for display purposes in order to show both positive and negative values.

III. RESULTS

Table II shows the MSE and bit rates per pixel for the CT and chest images using the FFBA compression technique both with and without splitting. Table III gives the same information using VQTSE. The MSE and bit rate for all CT images were computed inside a circle with a diameter of 512 pixels. When the splitting technique was used, the MSE of the full reconstructed image was the same as that of the R9LSB image, since the top 3MSB of the images were preserved without error. The average compression ratio using DPCM/LZ coding for the 3MSB of the CT images and chest radiographs was about 12:1.

A. Quantitative results of image splitting method

When used with FFBA, the splitting technique was ineffective in most cases. For the CT images, the bit rates per pixel obtained from splitting and nonsplitting were about the same; this was also true of the average MSE (20% of MSE increased and 20% of bit rate decreased by using the splitting method). For the larger ($1024 \times 1024 \times 12$) images chest 6 and chest 7, using the splitting technique even yielded slightly inferior results (on the average, 40% higher MSE and 15% lower bit rate when splitting technique was used). However, the effects of the splitting technique seem to be image dependent when used on the larger chest images. The results obtained for chest 6 by using splitting and nonsplitting methods were comparable, but for chest 7, nonsplitting gave better results than splitting.

However, the splitting technique did prove to be effective when used with FFBA on the smaller ($512 \times 512 \times 12$) chest image. Using the splitting technique resulted in a substantially lower MSE and lower bit rate per pixel (higher compression ratio) than when splitting was not used. In addition, when splitting was used with VQTSE, compression performance was vastly improved. The average MSE values obtained by splitting were lower than the values obtained by not splitting by a factor of 2.5.

Tables II and III also show the differences between the results of FFBA and VQTSE. With the CT abdominal im-

TABLE II. The global measurements and bit rates per pixel resulting from applying DPCM/LZ coding to the 3MSB images and FFBA to the R9LSB and the full 12-bit images.

Image #	MSE(w/split)	Total rate	[rate/pix(L9) + rate/pix(U3)]	MSE(no split)	Rate(no split)
18	219.051	1.337	(1.098 + 0.239)	350.633	1.024
25	249.624	1.468	(1.194 + 0.274)	292.379	1.108
26	143.348	1.963	(1.690 + 0.273)	266.158	1.232
27	150.079	1.935	(1.660 + 0.275)	242.854	1.486
28	171.158	1.795	(1.514 + 0.281)	164.069	1.940
29	260.116	1.462	(1.180 + 0.282)	157.646	2.056
30	404.742	1.089	(0.814 + 0.275)	149.400	2.078
31	385.584	1.223	(0.951 + 0.272)	168.404	2.084
32	387.316	1.198	(0.938 + 0.260)	123.416	2.709
33	228.122	1.601	(1.348 + 0.253)	124.239	2.559
34	282.470	1.290	(1.052 + 0.238)	170.384	1.758
35	167.804	1.584	(1.345 + 0.239)	155.030	1.877
36	122.256	1.661	(1.422 + 0.239)	133.951	1.989
37	200.947	1.300	(1.064 + 0.236)	183.021	1.528
38	126.766	1.753	(1.528 + 0.225)	175.460	1.710
39	225.315	1.213	(0.998 + 0.215)	182.022	1.532
40	264.172	1.106	(0.887 + 0.219)	166.799	1.334
Average	234.639	1.469	(1.217 + 0.253)	188.580	1.765
ctl(head)	317.546	1.516	(1.253 + 0.263)	216.516	0.525
chest1	274.839	0.665	(0.366 + 0.299)	509.786	1.120
chest6	238.089	0.602	(0.356 + 0.246)	248.899	0.505
chest7	329.991	0.553	(0.292 + 0.261)	152.636	0.523

Note: Images 18–40 were a set of abdominal CT images, "ct 1" was a single CT head image, "Chest 1" was a $512 \times 512 \times 12$-bit digitized chest radiograph, and Chest 6 and Chest 7 were $1024 \times 1024 \times 12$-bit radiographs digitized by a laser film scanner.

TABLE III. The global measurements and bit rates per pixel resulting from applying DPCM/LZ coding to the 3MSB images and VQTSE to the R9LSB and the full 12-bit images.

Image #	MSE(w/split)	Total rate	Training Sequence: CT images 20–24 (abdominal) [Rate/pix(L9) + rate/pix(U3)]	MSE(no split)	Rate(no split)
18	253.548	1.478	(1.239 + 0.239)	479.743	1.697
25	326.865	1.549	(1.275 + 0.274)	824.365	1.723
26	324.980	1.563	(1.290 + 0.273)	643.649	1.735
27	330.590	1.574	(1.299 + 0.275)	742.529	1.748
28	335.091	1.582	(1.301 + 0.281)	705.116	1.757
29	351.802	1.593	(1.311 + 0.282)	828.759	1.766
30	356.303	1.608	(1.333 + 0.275)	972.730	1.781
31	384.642	1.601	(1.329 + 0.272)	1116.812	1.777
32	383.532	1.608	(1.348 + 0.260)	1306.749	1.785
33	368.621	1.612	(1.359 + 0.253)	1227.316	1.794
34	336.420	1.583	(1.345 + 0.238)	1011.483	1.779
35	305.235	1.570	(1.331 + 0.239)	915.825	1.769
36	250.781	1.531	(1.292 + 0.239)	605.501	1.743
37	275.922	1.556	(1.320 + 0.236)	649.602	1.769
38	288.985	1.567	(1.342 + 0.225)	709.996	1.788
39	275.276	1.544	(1.329 + 0.215)	674.636	1.756
40	256.509	1.576	(1.357 + 0.219)	664.551	1.723
Average	317.947	1.570	(1.318 + 0.253)	828.196	1.758
ctl(head)	658.801	1.669	(1.406 + 0.263)	3788.342	1.865
chest1	1060.575	1.607	(1.308 + 0.299)	247 699.379	3.437

Training Sequence: chest images 1–5

Image #	MSE(w/split)	Total Rate	[Rate/pix(L9) + Rate/pix(U3)]
chest6	388.284	1.501	(1.255 + 0.246)
chest7	326.414	1.433	(1.172 + 0.261)

Note: Images 18–40 were a set of abdominal CT images. Images 20–24 were used to make the code book training sequence before applying VQTSE encoding to the images listed above (except chest 6 and chest 7). Chest 1 to chest 5 were used for the VQTSE training sequence for chest 6 and chest 7.

ages, FFBA and VQTSE attained similar bit rates per pixel. FFBA attained a lower MSE than VQTSE (about 75% of that for VQTSE with splitting and only 25% of that for VQTSE without splitting). FFBA also exhibited lower MSE and lower bit rates per pixel for CT head and chest images, both of which had been compressed using a CT abdominal image codebook library in VQTSE.

B. Qualitative results of image splitting method

Figure 2 shows the results of applying the FFBA technique: (a) the R9LSB of a sample chest image (image chest 6); (b) the reconstructed image resulting from applying FFBA compression to the R9LSB image; (c) the difference image between (a) and (b); (d) the full 12-bit original image; (e) the reconstructed image resulting from applying FFBA to the original 12-bit image; (f) the difference image between (d) and (e); (g) the 3MSB of the chest image; (h) the reconstructed image resulting from applying VQTSE to the R9LSB image; and (i) the difference image between (a) and (h). Figure 3 gives the corresponding results obtained by applying the VQTSE technique to a sample CT image (image 36). In Fig. 2, a gray value of 2048 was added to the R9LSB and its reconstructed images for display purposes. In Fig. 3, a wide range was applied to (d) and (e) so that differences in low CT values could be more easily observed.

As can be seen in both Figs. 2 and 3, the difference images obtained by using the image splitting method contain a less observable pattern than those obtained without using it. Although, as was discussed earlier, the MSE and bit rates for splitting and nonsplitting were comparable for FFBA, we see here that using the splitting method resulted in less structure in the difference images than using nonsplitting.

It appears that in the FFBA reconstructed images, small blurry artifacts are present around the edges of the images. On the other hand, in the VQTSE reconstructed images, one can observe jagged artifacts on the edge. Some small-block artifacts are apparent in the VQTSE images as well. Observation of the difference images from both techniques reveals that the VQTSE difference images contain more structured information than the FFBA difference images. Lines and round shapes can be seen in the difference images when using FFBA for the full 12-bit chest radiograph and for the full 12-bit CT abdominal image, respectively. These patterns are eliminated by using FFBA and the splitting technique.

IV. CONCLUSIONS AND DISCUSSION

In this study, the experiments were conducted first by using DPCM/LZ coding for the top 3MSB, and FFBA and VQTSE for the R9LSB (splitting method), and second, by using FFBA and VQTSE on the full 12-bit data (nonsplitting method). The splitting technique requires two more processes than nonsplitting both for compression and for decompression. For compression, splitting and remapping

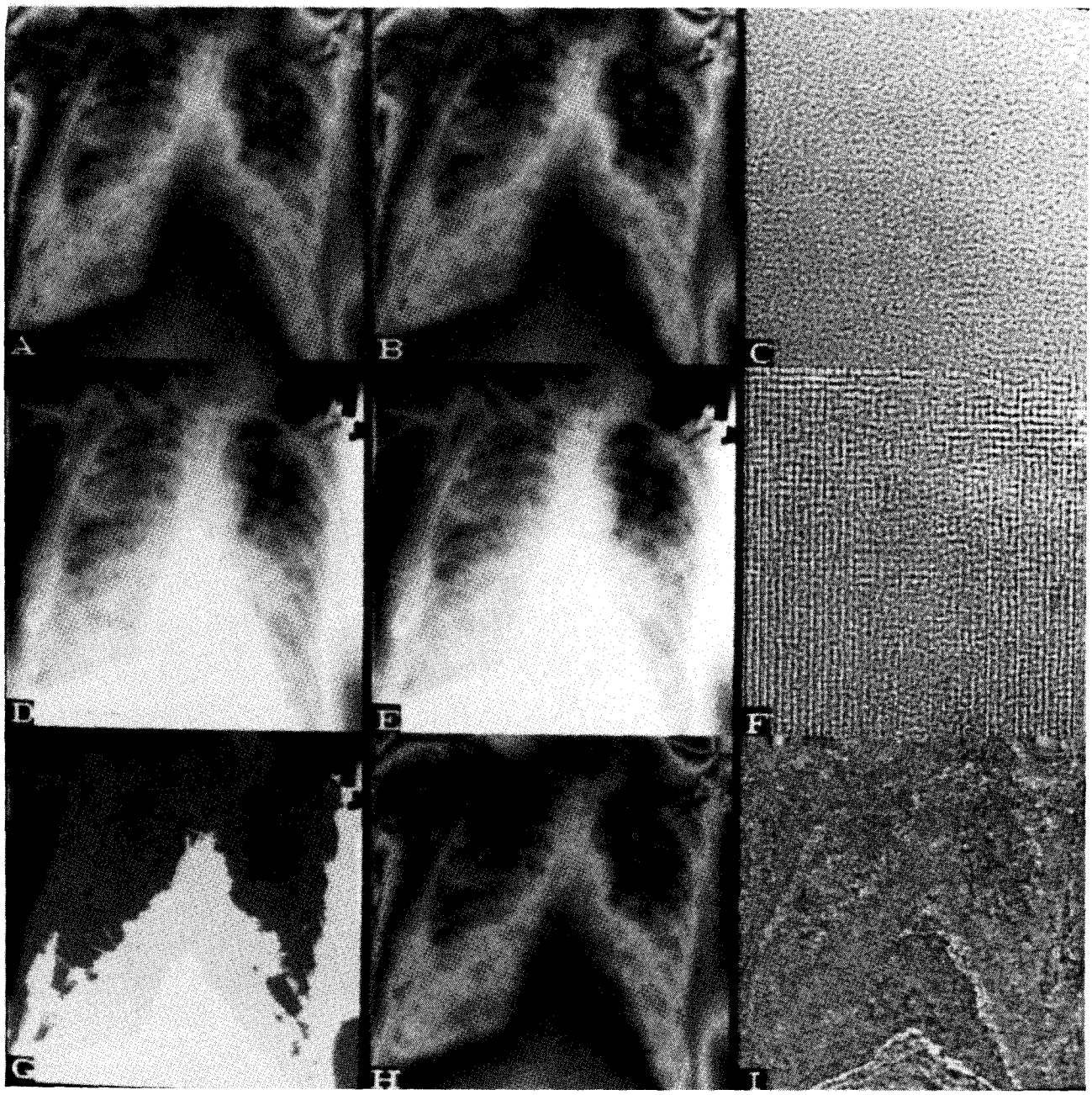

FIG. 2. (a) the R9LSB of a sample chest image (image chest 6); (b) the reconstructed image resulting from applying FFBA compression to the R9LSB image; (c) the difference image between (a) and (b); (d) the full 12-bit original image; (e) the reconstructed image resulting from applying FFBA to the original 12-bit image; (f) the difference image between (d) and (e); (g) and 3MSB of the chest image; (h) the reconstructed image resulting from applying VQTSE to the R9LSB image; and (i) the difference image between (a) and (h).

can be done very quickly; the DPCM/LZ coding also take very little time to process. This is also true for 3MSB decompression and rejoining of pixel values from 3MSB and R9LSB. We used a SUN 3/260 for the compression study, and the software was written in C. For a 512×512 image, it took about 5 min for FFBA and 6 s for DPCM/LZ coding.

We chose to use the proposed splitting technique because of its ability to (a) prevent errors in encoding for the most significant bits and (b) lessen edge artifacts caused by compression and decompression procedures. The technique proved to be effective when used on the small ($512 \times 512 \times 12$) chest image, which contained a sharp strip edge between the film edge and the air on the left margin. This is due to the fact that FFBA is sensitive to sharp strips, especially with small size image compression. The proposed remapping method for the lower bit image also showed significant improvement when used in the VQTSE technique. The reason for this is that the predictive accuracy of the VQ library is more effective for a smaller than for a larger value range. In addition, the R9LSB of the images are generally

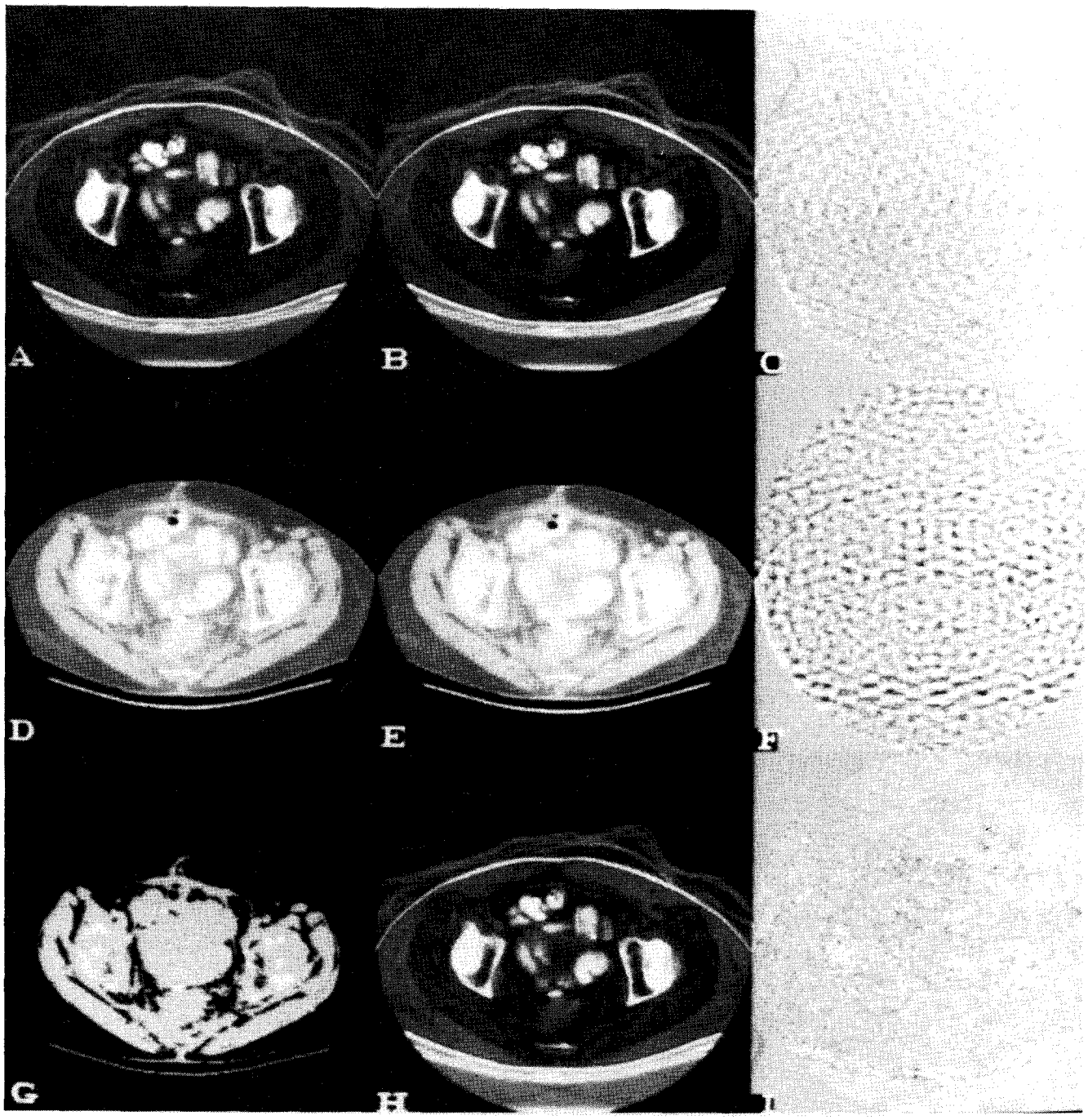

FIG. 3. Same image sequence as Fig. 2 with a CT abdominal image. (a) the R9LSB of a sample CT image (image 36 in the CT set); (b) the reconstructed image resulting from applying FFBA to the R9LSB image; (c) the difference image between (a) and (b); (d) the full 12-bit original image; (e) the reconstructed image resulting from applying FFBA to the original 12-bit image; (f) the difference image between (d) and (e); (g) the 3MSB of the CT image; (h) the reconstructed image resulting from applying VQTSE to the R9LSB image; and (i) the difference image between (a) and (h).

smoother than the original image, which means that more information is concentrated in the low-frequency portion of the 2-D–DCT. However, the advantage of taking the 2-D–DCT characteristics in the RLSB image can be offset by the overhead required in the compression of the MSB image. In fact, this was found to be the case when testing one of the $1024 \times 1024 \times 12$ chest radiographs, chest 7.

Since vector quantization requires training procedures using a series of the same type of image to make its codebook libraries, an image of a type other than the training sequence cannot be encoded and reconstructed with sufficient quality. A training sequence of CT abdominal images, when applied to a chest radiograph, produced an unacceptable reconstructed image; on the other hand, when it was applied to a CT head image, the reconstructed image did not show obvious artifacts with an intermediate compression ratio (e.g.,

5:1). However, it is expected that a training sequence of CT head images would yield even better results. In both cases, the performance was not quite as good as that of FFBA.

From this study, it seems that FFBA generally produced better results for MSE and bit rate per pixel than VQTSE. However, this is not the main research perspective of this paper. The authors use the techniques (FFBA for frequency quantization and VQTSE for spatial quantization) only as examples in order to evaluate the effects of the image splitting technique proposed here. Although FFBA with the splitting technique does not always produce the best bit rate result, it can be applied to any image, without preprocessing for sharp edges. With this technique, one can obtain a reconstruction image without edge effects and a high compression ratio. FFBA may require more computation than VQTSE, especially for a larger-size image (one greater than 1024×1024). VQTSE, on the other hand, may lead to some difficulty in categorizing codebook libraries for practical use. In Refs. 3 and 4, the research showed that the larger the image size, the better the results from the FFBA technique. However, this was not the case with VQTSE.

The CT head image consists of sharp edges between air and skull (CT value ≈ -1000 and ≈ 1000) and between brain and skull (CT value ≈ 0 and ≈ 1000). Both the VQ and FFBA techniques could have difficulty with this type of image.[5,11] If the skull is extracted from the image, FFBA can be a good compressor, with a compression ratio of 10:1.[4] However, this is not a simple operation for CT images composed of temporal bones. A possible remedy for handling sharp-edge images is the proposed splitting method, which reduces the edge problem in a simple way.

Depending on the characteristics of the source image, the encoding may or may not be favorable to the MSB and RLSB images. It would be desirable to explore a new error-free compression technique for MSB images. Once we can reduce the bit rate of 3MSB images to less than 0.1 bit/pixel, the total number of bits per pixel obtained by using the splitting method with the same MSE will be decreased by 10% to 25%, based on Table II. In our preliminary studies, we tried using run-length/Huffman coding on the 3MSB images, but our compression results were comparable to those obtained by using DPCM/LZ coding.

In this paper, we used MSE and difference image to evaluate the difference between original and reconstruction images. MSE is a global measurement of the difference in the images and does not show the characteristics of the differences. The difference image shows the variance in each pixel qualitatively. Neither method is an optimal way of comparing the reconstruction image to the original image. In a way, however, the two methods complement each other. In both Figs. 2 and 3, one can see that the difference image with splitting in (c) contains more structure from the high-frequency regions and the difference image without splitting in (i) contains more structure from the low-frequency regions. However, the MSEs are comparable in both cases.

In conclusion, the use of the splitting technique was seen to improve the performance of VQTSE drastically and produce less artifacts in the reconstruction images for FFBA in our experiments. It is anticipated that research on other advanced coding techniques[12,13] (e.g., predictive VQ) will progress rapidly, and further investigation will be needed in order to evaluate the effects of incorporating the proposed splitting and remapping method with these techniques.

ACKNOWLEDGMENTS

This work is supported in part by the US Army Medical Research Acquisition Activity of the US Army Medical Research and Development Command Contract No. DAMD 17-86-C-6145. The views and opinions contained in this document are those of the authors and should not be construed as official Department of Army position, policy, or decision unless so designated by other documents. The authors are grateful to Dr. Eve Riskin for providing the VQTSE software use in this study. Acknowledgment is also extended to the reviewers for their constructive comments in improving the paper.

[1] R. K. Taira, N. J. Mankovich, M. I. Boechat, H. Kangarloo, and H. K. Huang, "Design and implementation of a picture archiving and communication system for pediatric radiology," Am. J. Radiol. **150**, 1117–1121 (1988).

[2] S. C. Lo and H. K. Huang, "Radiological image compression: Full-frame bit-allocation technique," Radiology **155**, 811–817 (1985).

[3] S. C. Lo and H. K. Huang, "Compression of radiological images with matrix sizes 512, 1024, and 2048," Radiology **161**, 519–525 (1986).

[4] S. C. Lo, "Radiological image compression," Ph.D. Thesis, UCLA, Los Angeles, CA (1986).

[5] E. A. Riskin, T. Lookabaugh, P. A. Chou, and R. M. Gray, "Variable rate vector quantization for medical image compression," IEEE Trans. Med. Imag. **9**(3), 290–298 (1990).

[6] T. Lookabaugh and R. M. Gray, "High-resolution quantization theory and vector quantizer advantages," IEEE Trans. Inform. Theor. **IT-35**, 1020–1033 (1989).

[7] J. Ziv and A. Lempel, "An universal algorithm for sequential data compression," IEEE Trans. Inform. Theor. **IT-23**, 337–343 (1977).

[8] D. A. Huffman, "A method for the construction of minimum redundancy codes," Proc. IRE **6**, 7–12 (1953).

[9] S. C. Lo, B. Krasner, and S. K. Mun, "Noise impact on error-free image compression," IEEE Trans. Med. Imag. **9**(2), 202–206 (1990).

[10] S. C. Lo, J. W. Gaskill, S. K. Mun, and B. H. Krasner, "Contrast information of digital imaging in laser film digitizer and display monitor," J. Dig. Imag. **3**(2), 119–123 (1990).

[11] K. K. Chen, S. L. Lou, and H. K. Huang, "Full-frame transform compression of CT and MR images," Radiology **171**, 847–851 (1989).

[12] H. Hang and J. W. Woods, "Predictive vector quantization of images," IEEE Trans. Acoust. Speech Signal Process. **ASSP-33**, 1208–1219 (1985).

[13] P. A. Chou, T. Lookabaugh, and R. M. Gray, "Entropy-constrainted vector quantization," IEEE Trans. Acoust. Speech Signal Process. **ASSP-37**, 31–42 (1989).